

Pressure-induced effects in the spectra of collective excitations in pure liquid metals

Taras Bryk^{1,2,5}, Taras Demchuk¹, Jean-François Wax³ and Noël Jakse⁴

¹ Institute for Condensed Matter Physics of the National Academy of Sciences of Ukraine,
1 Svientsitskii Street, UA-79011 Lviv, Ukraine

² Lviv Polytechnic National University, UA-79013 Lviv, Ukraine

³ Laboratoire de Chimie et de Physique A2MC, Université de Lorraine, Metz, 1, boulevard Arago 57078
Metz Cedex 3, France

⁴ Université Grenoble Alpes, CNRS, Grenoble INP, SIMaP, F-38000 Grenoble, France

E-mail: bryk@icmp.lviv.ua

Received 23 October 2019, revised 13 December 2019

Accepted for publication 10 January 2020

Published 4 February 2020



Abstract

Collective dynamics of metallic melts at high pressures is one of the open issues of condensed matter physics. By means of *ab initio* molecular dynamics simulations, we examine features of dispersions of collective excitations through transverse current spectral functions, as a function of pressure. Typical metallic melts, such as Li and Na monovalent metals as well as Al, Pb and In polyvalent metals are considered. We firmly establish the emergence of a second branch of high-frequency transverse modes with pressure in these metals, that we associate with the pronounced high-frequency shoulder in the vibrational density of states. Similar correlation also exist with the low frequency modes. The origin of the pressure-induced evolution of transverse excitations in liquid metals is discussed.

Keywords: liquid metals, collective excitations, *ab initio* simulations

(Some figures may appear in colour only in the online journal)

1. Introduction

One of the important and yet open issues in condensed matter physics is the collective dynamics in liquids and more specifically in liquid metals and alloys on mesoscopic and molecular length-scales [1–3]. Longitudinal acoustic-like collective modes are well-defined excitations with small damping in the liquid on the macroscopic length-scale because of the hydrodynamic mechanism of sound propagation, which is governed by local conservation laws. Both density and momentum density fluctuations in liquids belong to the fluctuations of conserved quantities, and their two coupled balance equations result in long-wavelength limit in wave solutions with typical hydrodynamic behavior of acoustic modes: linear dispersion law ck and quadratic damping Γk^2 , where k is wave-number, c and Γ are macroscopic speed of sound and damping coefficient,

respectively. One can see that the damping (inverse lifetime of the excitation) decreases for $k \rightarrow 0$, that is the typical feature of hydrodynamic processes to have their lifetime $\sim k^{-2}$.

This is not the case for transverse collective excitations, also called shear waves, which belong to non-hydrodynamic modes [3]. For the case of transverse dynamics, the only conserved quantity that exists is the transverse component of total momentum, and a single balance equation (first order differential equation) for the density of transverse momentum can never result in a wave-like solution. That is why macroscopic transverse sound does not exist in liquids. Only outside the hydrodynamic regime, when the lifetimes of hydrodynamic and non-hydrodynamic processes become comparable, the short-wavelength transverse propagating modes can emerge due to coupling of fluctuations of transverse components of momentum and stress tensor [3]. The same mechanism of propagating modes exists also for longitudinal high-frequency acoustic modes (high-frequency sound), when coupled fluctuations of longitudinal components of stress-tensor

⁵ Author to whom any correspondence should be addressed.

and momentum density appear. And, actually the viscoelastic transition of liquids, has the sense of transition from hydrodynamic (based on conservation laws) to elastic mechanism of sound propagation [4]. The latter is solid-like because it involves the microscopic forces between particles (which enter the stress-tensor components), while in hydrodynamic mechanism atomistic structure is not relevant. In general, the transition from hydrodynamic to high-frequency sound (positive sound dispersion) and emergence of shear waves are two related manifestations of the viscoelastic transition, although the onset of the positive sound dispersion takes place typically at much smaller wavenumbers than the value of the propagation gap for transverse excitations [5].

Although transverse excitations do not directly contribute to the dynamic structure factors, there were reports on inelastic x-ray scattering (IXS) experiments on liquid Na [6] and polyvalent liquid metals such as Ga [7] and Sn [8], in which fitting the experimental scattering intensity allowed to obtain small contributions from transverse excitations. In this sense computer simulations allow to obtain more insight in transverse dynamic processes in liquids. Recent findings based on atomistic simulations of liquid Li [9], Na [10] and Fe [11] at high pressures indicate the possible emergence of unusual second high-frequency contribution to transverse spectral functions that coexists on the spatial scale of neighboring cage around atoms. Triggered by this intriguing feature, it has been shown very recently that they might also exist for some metals at ambient pressure [12, 13], though these two modes can display significant overlap [14].

This emerging picture of transverse collective excitations in liquid metals from the recent contributions prompts us for further studies on this issue. As a matter of fact, the question about its general applicability for all liquid metals and their alloys remains open. Furthermore, no consensus exists about its origin. It has been suggested that the emergence of transverse modes comes from contributions of the longitudinal ones [15, 16], following a relationship between the L- and T-current spectral functions based on mode-coupling approach. Such an emergence of contributions from longitudinal excitations in the transverse spectral functions was revealed and documented in simulations of water [17, 18]. For liquid metals, it has been shown [12–14] that the high frequency transverse modes coincide with the simultaneous emergence of a high frequency peak in the vibrational density of states.

The present work is devoted to the study of the pressure evolution of the collective dynamic properties of liquid sodium and indium, which are typical of monovalent and polyvalent metals, respectively. To this end, we have performed a series of *ab initio* molecular dynamics (AIMD) simulations for pressures ranging from ambient pressure up to 147 GPa for Na and 10 GPa for In. While for Na, the simulations were done for thermodynamic states along an isotherm above the temperature maximum of the melting line, for In the simulations follow this line. The major advantage in using AIMD is to ensure transferability of interactions as a function of temperature and pressure that could not be obtained for effective

Table 1. Thermodynamic state points for all the simulations for Na and In.

Na					
T (K)	893	893	393	893	893
P (GPa)	15	83	116	116	147
ρ (\AA^{-3})	0.0514	0.0889	0.1000	0.1000	0.1093
In					
T (K)	443	600	750		
P (GPa)	0	4.4	9		
ρ (\AA^{-3})	0.0387	0.0419	0.0443		

atom-atom interactions [19] in strongly non-uniform electron density situations encountered for such extreme conditions. We examine the dynamics through the vibrational density of states (VDOS) obtained via the spectrum of the velocity auto-correlation function (VACF) as well as the dispersion of transverse (T) collective excitations analyzed through the T-current spectral functions. Our results show the emergence of a second branch of high-frequency T-modes for all pressures. Moreover, we confirm the coincidence of VDOS peak locations with these two transverse collective modes for these two metals. Including here our results for Li [9], Al [14] and Pb [13] as well as those of Fe [11], we find for all metals a strong linear correlation between transverse collective modes and the number density. This linear behavior holds for the two transverse branches and have a different slope for monovalent and polyvalent metals.

2. Computational background

The dynamics of liquid Na and In as a function of pressure is investigated from AIMD simulations within the density-functional theory (DFT) using the Vienna *ab initio* simulation package [20, 21]. A plane-wave basis has been set with the standard energy cutoff, namely 259.6 eV for Na and 95.9 eV for In. The projected augmented-wave method [22, 23] has been used to describe the electron-ion interactions. Seven electrons ($2p^63s^1$) have been taken into account with the local density approximation (LDA) [24, 25] of exchange-correlation energy for Na similarly, as we used in the case of liquid Na at ambient pressure in order to get better agreement with experimental data [26], and 3 valence electrons with the generalized gradient approximation (GGA) in PBE [27] formulation for In.

The simulations were performed in the canonical ensemble (NVT), namely constant number of atoms, volume, and temperature, by means of a Nosé thermostat [28, 29]. Newton's equations of motion were integrated using Verlet's algorithm in the velocity form with a time step of 3 fs for Na and 2 fs for In. Since in the case of Na we faced much larger computational efforts because of 1200 electron bands in simulations, we used for Na a little bit larger time step than for liquid In. Cubic simulation supercells with periodic boundary conditions containing 300 atoms for both metals were used,

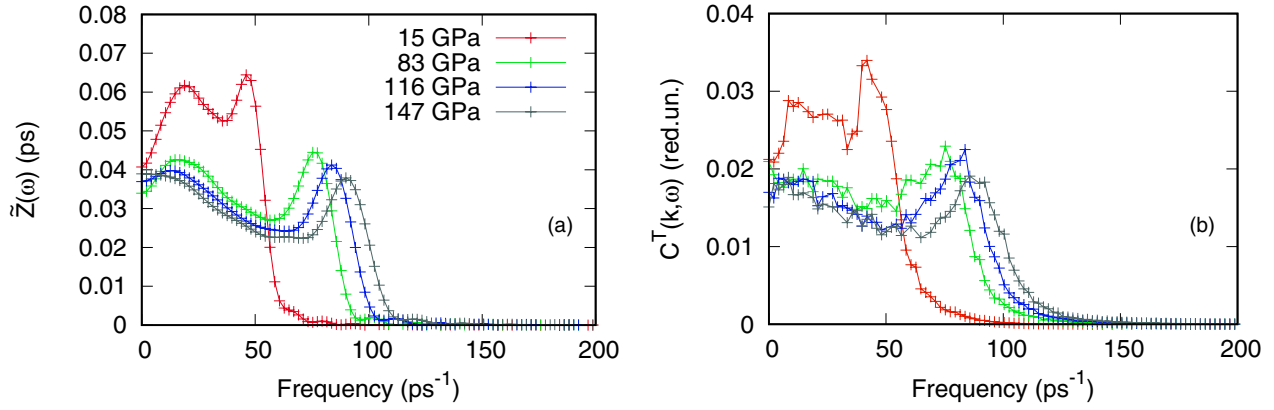


Figure 1. Liquid sodium at 893 K: (a) vibrational density of states, (b) spectral density of the transverse current correlation functions $C^T(k, \omega)$ for wave numbers k between 2.09 and 2.69 \AA^{-1} for all pressures.

and only the Γ -point sampling was considered to sample the supercell Brillouin zone, that was justified by quite large size of the studied systems.

For both systems, liquid samples were prepared from a random configuration, whose size was fixed to get the smallest target pressure, and run for 12 ps for Na and 6 ps for In at the temperature studied until thermal equilibrium was reached. Then, for the thermodynamic states at higher pressures, the volume V of cell was adjusted manually to reach the higher pressures for Na on the studied isotherm and subsequently equilibrated in NVT ensemble. For In, additionally, the temperature was progressively adjusted to fall just above the experimental melting line. The data of respective temperatures, pressures and densities can be found in table 1. After equilibration, runs were subsequently continued for 60 ps for Na and 46 ps for In to extract all the physical properties. For the other metals considered in the present work, Li, Al, Fe, Pb, the simulation procedure and thermodynamic parameters can be found in the corresponding contributions.

Here, we focus on the vibrational density of states that stems from an analysis of the single-particle dynamics, and more specifically the VACF

$$\Psi(t) = \frac{1}{N} \left\langle \sum_{i=1}^N [\mathbf{v}_i(t + t_0) \cdot \mathbf{v}_i(t_0)]^2 \right\rangle_{t_0}, \quad (1)$$

where $\mathbf{v}_i(t)$ denotes the velocity of atom i at time t . The angular brackets correspond to an averaging over time origins t_0 . The VDOS is then determined as the time Fourier transform of the normalized VACF $\Psi_N(t) = \Psi(t)/\Psi(t = 0)$

$$\tilde{Z}(\omega) = \int_0^\infty \Psi_N(t) \cos(\omega t) dt. \quad (2)$$

As central quantities of this work, we consider both the longitudinal and transverse collective excitations obtained from the Fourier-spectra of the corresponding L- and T-current time correlation functions. The time correlation functions were calculated from the simulation data using the relations:

$$\begin{aligned} F_{JJ}^{L/T}(k, t) &= \langle \mathbf{J}_{L/T}(-k, t) \mathbf{J}_{L/T}(k, 0) \rangle, \\ \mathbf{J}_{L/T}(k, t) &= \frac{1}{\sqrt{N}} \sum_{i=1, N} \mathbf{v}_{i, L/T}(t) e^{-i\mathbf{k}\mathbf{r}_i(t)} \end{aligned} \quad (3)$$

where $\mathbf{v}_{i, L/T}(t)$ is the L (along the direction of wave vector \mathbf{k}) or T-projection (in the plane perpendicular to the direction of wave vector) of particle velocity. We have to mention, that all the time correlation functions were averaged over all possible directions of wave-vectors \mathbf{k} having the same absolute value, and all the sampled wave-vectors were compatible with the simulation box size. Since the size of the simulation box is not constant in the constant pressure ensemble (NPT) one cannot apply NPT simulations in the study of k -dependent quantities of collective dynamics.

3. Results and discussion

We first consider the single-atom dynamics through the VDOS, $\tilde{Z}(\omega)$, that has been calculated from the Fourier transform of the VACF, using equation (2). $\tilde{Z}(\omega)$ are shown in figures 1(a), 2(a), 3(a) and 4(a) for Na, In, Pb, and Al, respectively, and for all studied pressures. The low frequency limit of $\tilde{Z}(\omega)$ takes a non zero value that is related to the self-diffusion coefficient, showing that the studied systems are in the liquid state for given pressures. As the frequency increases, all studied metals share similar features under pressure, namely two peaks of the $\tilde{Z}(\omega)$ that shift towards higher frequencies with increasing pressure. Since the time-Fourier transformation of current-current time correlation functions from AIMD is usually very noisy in order to reduce the error bars in the estimation of the observed peak position one usually applies a fit with the chosen (Lorentzian, damped harmonic oscillator or Gaussian) function of frequency. While the high-frequency peak has been obtained by simply fitting the raw data by a Gaussian, the low-frequency peak has been obtained by an analysis of the VDOS in terms of the two phase thermodynamic (2PT) [31] model [14]. Moreover, the difference between the low- and high-frequency peaks increase with pressure. At ambient pressure, the VDOS clearly shows two peaks for indium and lead, while for sodium and aluminium it displays a broad single peak, with even a shoulder in the case of Al. A more detailed analysis for these two metals indicates that the broad peak can be decomposed into two contributions of low- and high-frequency mode with a significant overlap [14, 30].

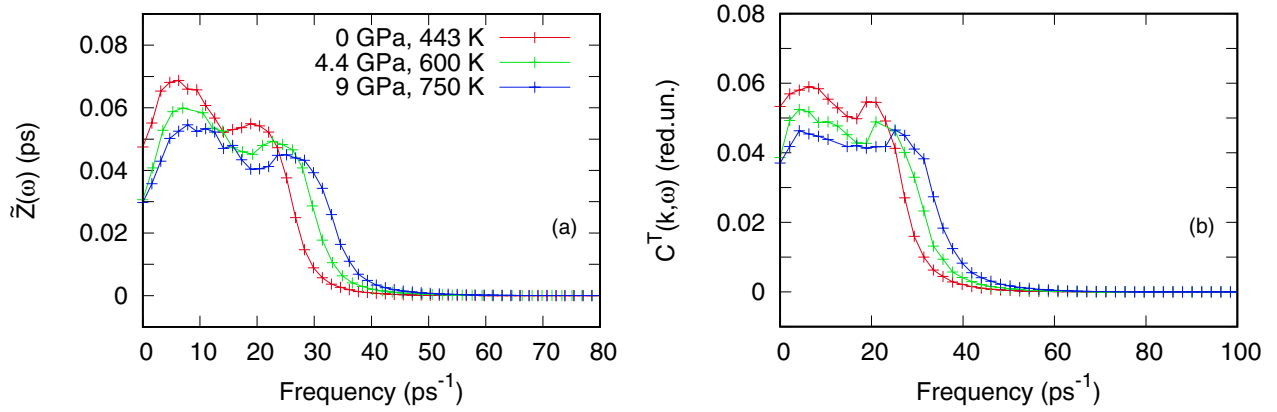


Figure 2. Liquid indium along the melting line: (a) vibrational density of states, (b) spectral density of the transverse current correlation functions $C^T(k, \omega)$ for wave numbers k between 2.48 and 2.49 \AA^{-1} for all pressures.

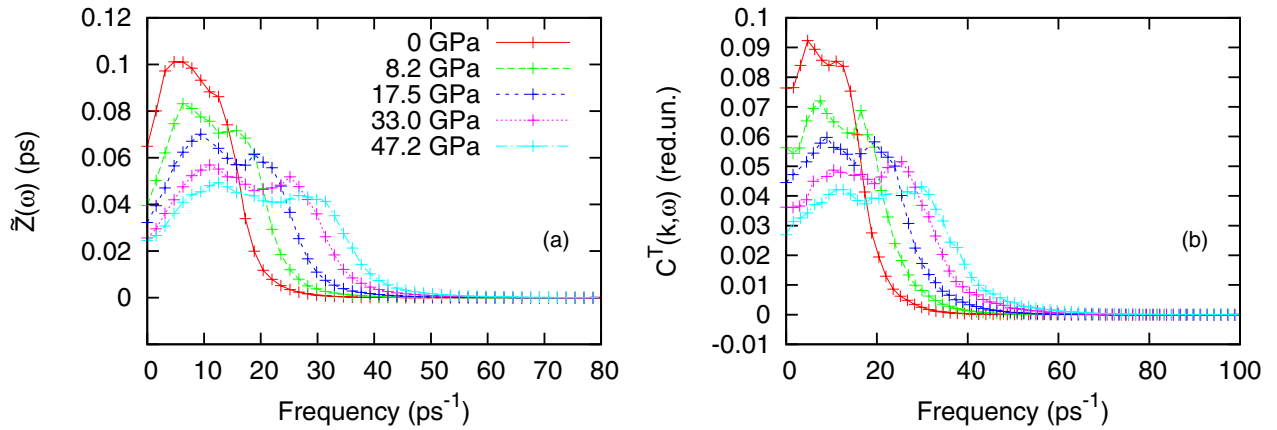


Figure 3. Liquid lead along the melting line: (a) vibrational density of states, (b) spectral density of the transverse current correlation functions $C^T(k, \omega)$ for wave numbers k between 2.28 and 2.30 \AA^{-1} for all pressures.

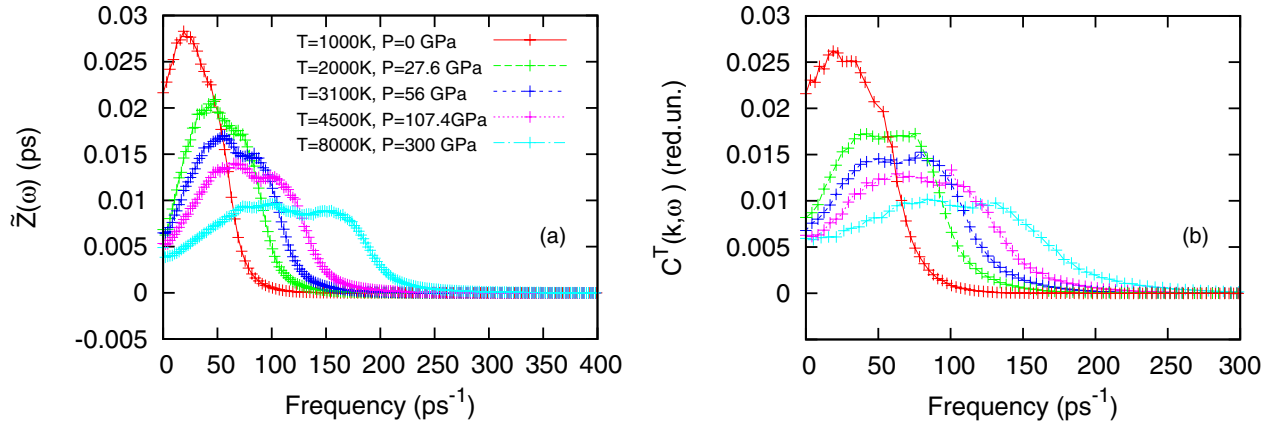


Figure 4. Liquid aluminium along the melting line: (a) vibrational density of states, (b) spectral density of the transverse current spectral functions $C^T(k, \omega)$ for wave numbers k between 2.34 and 2.36 \AA^{-1} for all pressures.

In order to rationalize such a two-mode structure in the VDOS and to relate it to collective modes, we have determined the spectral density of the transverse current correlation functions $C^T(k, \omega)$, from the numerical time-Fourier transformation of the corresponding transverse current auto-correlation functions $F_{JJ}^{L/T}(k, t)$ given by equation (3) for each available wave number compatible with the size of the simulation cells. The existence and propagative nature of these two transverse

modes can be obtained from their dispersion curves, namely the evolution of maxima positions of $C^T(k, \omega)$ versus wave number. It was shown [13, 14, 30] that both T-collective excitations exist for wave numbers higher than the boundary of the first pseudo-Brillouin zone for all pressures. Moreover, the two transverse branches are almost flat, showing their non-propagative nature in the second pseudo-Brillouin zone. The spectral functions $C^T(k, \omega)$ for Na, In, Pb, and Al, are shown at

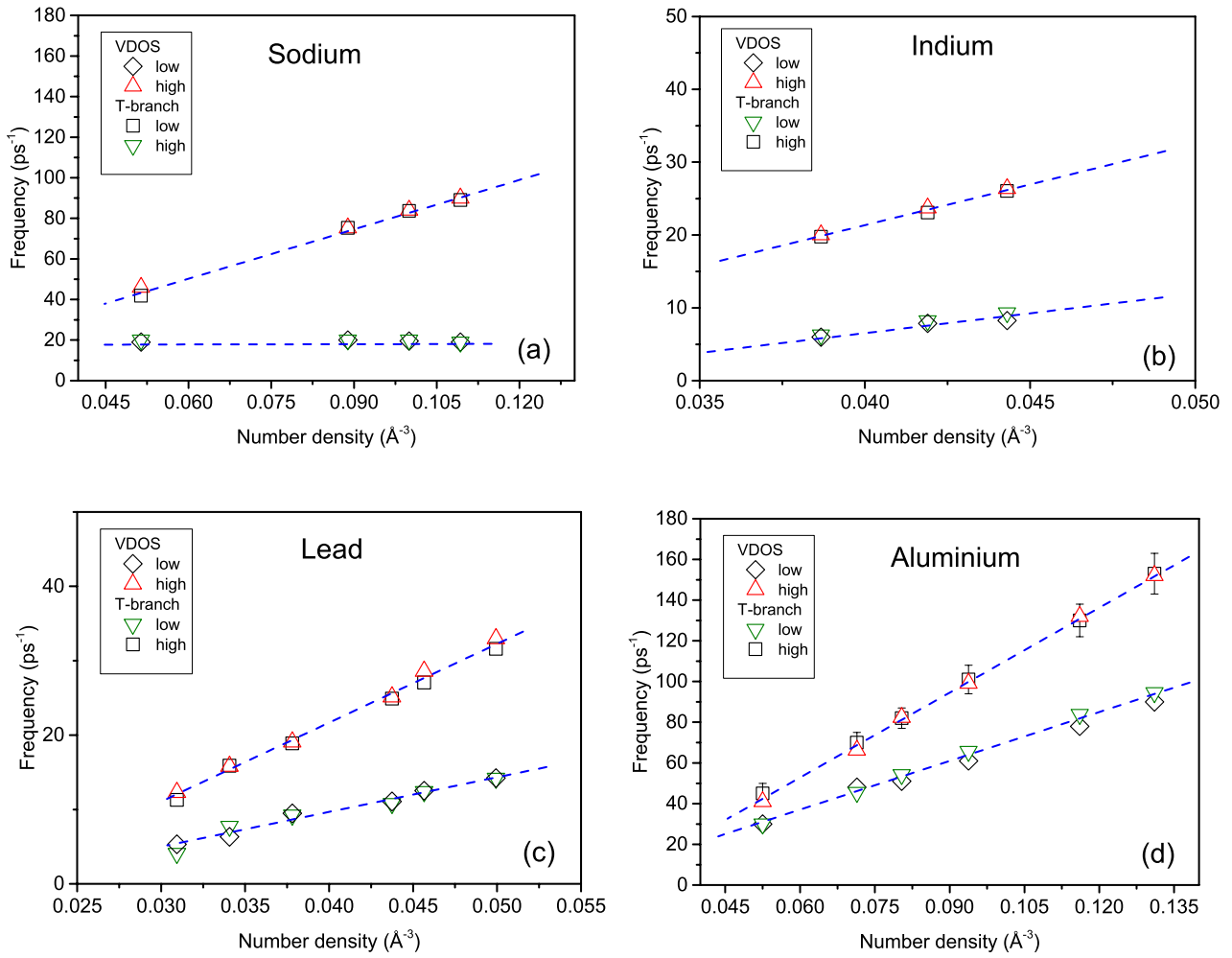


Figure 5. Low and high frequency transverse mode as a function of density from the transverse current spectra functions as well as for the frequency peaks of $\tilde{Z}(\omega)$: (a) Sodium, (b) Indium, (c) Lead, and (d) Aluminium.

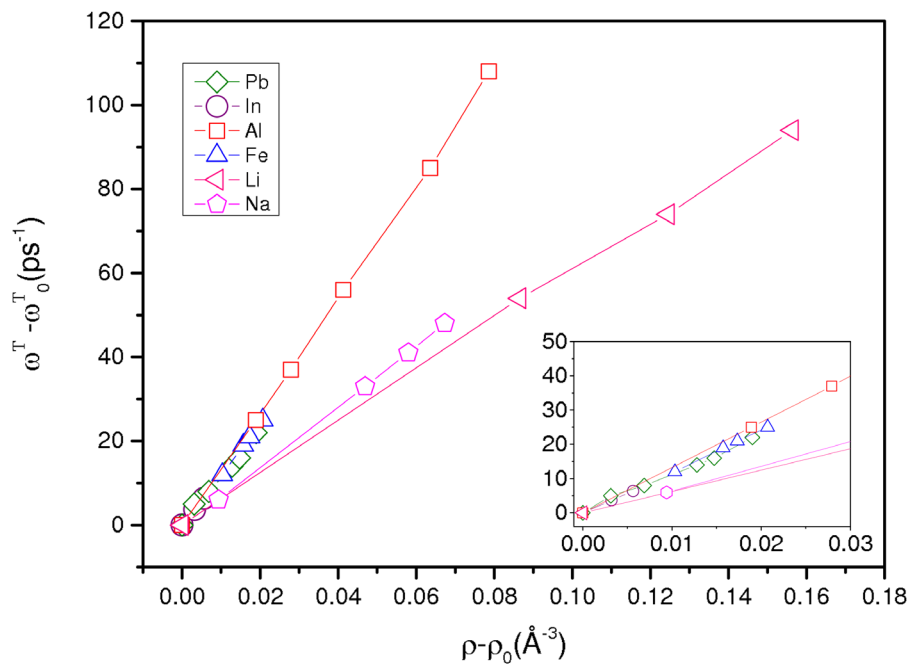


Figure 6. Transverse current spectral functions $C^{L,T}(k, \omega)$ high frequency modes as a function of the number density. Densities and frequencies are shifted with their values at ambient pressure. Inset: same as the main panel for the low density and frequency range.

comparable wave number in figures 1(b), 2(b), 3(b) and 4(b), respectively. Under pressure, $C^T(k, \omega)$ clearly shows a two peak shape which maxima become more and more separated with increasing pressure like in the VDOS shown in panels (a). At ambient pressure, for Na and Al, $C^T(k, \omega)$ displays a well-defined peak followed by a pronounced shoulder indicating an overlap of low- and high-frequency modes [14, 30].

In figure 5, the evolution with density of the low- and high-frequency maxima of the VDOS are compared to those of $C^T(k, \omega)$ in the flat region. For all studied metals, a strong coincidence of both maxima positions of $C^T(k, \omega)$ and VDOS is seen whatever the density, indicating undoubtedly a strong correlation between the single-particle dynamics and collective dynamical quantities. Moreover, they show similar linear evolution with density, with the low-frequency modes having a weaker slope.

As similarity in the density evolution of the transverse excitations exists, we have compared in figure 6 the high frequency transverse mode for all metals studied here as well as for liquid Fe and Li found in the literature [3, 11]. The data for the densities and frequencies have been shifted respectively with ρ_0 and ω_0 , the values of the density and frequency mode at ambient pressure. Strikingly, all the results fall on master curves for polyvalent metals and alkali metals, implying a possible universal behavior.

4. Conclusion

In this study, we aimed at analysis of general tendencies in transverse dynamics of liquid metals in a wide range of pressures. Recently, it was found that transverse spectral functions of dense metallic liquids like Li, Zn, Ni, Fe, Tl contain a high-frequency peak/shoulder in addition to the traditional peak corresponding to shear waves. By means of *ab initio* simulations we calculated vibrational density of states via the velocity autocorrelation functions, and spectra of collective transverse excitations in liquid Na and polyvalent liquid metals Al, Pb and In over a wide range of pressure.

We found the existence of the high-frequency peak/shoulder on transverse spectral functions in all the studied liquid metals for wave numbers beyond the first pseudo-Brillouin zone. A direct correlation was observed between the frequencies of the high-frequency peak/shoulder of the $C^T(k, \omega)$ and of the high-frequency feature of the vibrational density of states. We found, that a strong linear correlation with density exists for locations of the low- and high-frequency features of the transverse spectral functions for all studied metals, that can be a signature of a universal behavior in transverse dynamics. Still the mechanism of emergence of the second contribution to the transverse spectral function $C^T(k, \omega)$ remains unclear. Even if the high-frequency branch observed in transverse dynamics comes from the nonlocal L-T coupling [15] it is not clear what kind of microscopical processes leads to this coupling. In water, for example, the rotational motion of the polar molecular units immediately leads to the coupled L-T dynamics. That is why one of the possibilities for the coupled L-T dynamics in the

compressed metals can be emergence of short-lifetime associates, which can be the source of local vorticities leading to the coupled L-T dynamics of atomic length-scale. In any case, we expect that new features of the transverse dynamics reported in this study will be helpful in solving the puzzle of the microscopic dynamics on microscopic length-scales.

Acknowledgment

The calculations have been performed using the *ab initio* total-energy and molecular dynamics program VASP (Vienna *ab initio* simulation program) developed at the Institute für Materialphysik of the Universität Wien. We also acknowledge the CINES and IDRIS under Project N INP2227/72914, Joint French–Ukrainian project M/70-2019 under the ‘Dnipro’ program, PMMS (Pôle Messin de Modélisation et de Simulation), as well as CIMENT/GRICAD for computational resources. This work was performed within the framework of the Centre of Excellence of Multifunctional Architected Materials ‘CEMAM’ ANR-10-LABX-44-01 funded by the ‘Investments for the Future’ Program. TD benefited from new courses on AIMD of the ICMP PhD program developed in frames of DocHub/Erasmus+ project 574064-EPP-1-2016-1-LT-EPPKA2-CBHE-SP.

ORCID iDs

Taras Bryk  <https://orcid.org/0000-0002-4360-0634>
 Taras Demchuk  <https://orcid.org/0000-0002-3016-4909>
 Jean-François Wax  <https://orcid.org/0000-0003-2209-8427>
 Noël Jakse  <https://orcid.org/0000-0002-4031-0965>

References

- [1] Hansen J-P and McDonald I R 2006 *Theory of Simple Liquids* 3rd edn (London: Academic)
- [2] Bryk T and Mryglod I 2000 *J. Phys.: Condens. Matter* **12** 6063
- [3] Bryk T 2011 *Eur. Phys. J. Spec. Top.* **196** 65
 Bryk T 2019 *Eur. Phys. J. Spec. Top.* **227** 2689
- [4] Bryk T, Mryglod I, Scopigno T, Ruocco G, Gorelli F and Santoro M 2010 *J. Chem. Phys.* **133** 024502
- [5] Boon J-P and Yip S 1980 *Molecular Hydrodynamics* (New York: McGraw-Hill)
- [6] Giordano V M and Monaco G 2010 *Proc. Natl Acad. Sci. USA* **107** 21985
- [7] Hosokawa S *et al* 2009 *Phys. Rev. Lett.* **102** 105502
- [8] Hosokawa S, Munejiri S, Inui M, Kajihara Y, Pilgrim W-C, Ohmasa Y, Tsutsui S, Baron A Q R, Shimojo F and Hoshino K 2013 *J. Phys.: Condens. Matter* **25** 112101
- [9] Bryk T, Ruocco G, Scopigno T and Seitsonen A P 2015 *J. Chem. Phys.* **143** 110204
- [10] Marqués M, González D J and González L E 2016 *Phys. Rev. B* **94** 024204
- [11] Marqués M, González L E and González D J 2016 *J. Phys.: Condens. Matter* **28** 075101
- [12] Bryk T, Demchuk T, Jakse N and Wax J-F 2018 *Frontiers Phys.* **6** 6
- [13] Bryk T, Demchuk T and Jakse N 2018 *Phys. Rev. B* **99** 014201

- [14] Jakse N and Bryk T 2019 *J. Chem. Phys.* **151** 034506
- [15] del Rio B G and González L E 2017 *Phys. Rev. B* **95** 224201
- [16] del Rio B G, Chen M, González L E and Carter E A 2018 *J. Chem. Phys.* **149** 094504
- [17] Sampoli M, Ruocco G and Sette F 1997 *Phys. Rev. Lett.* **79** 1678
- [18] Bryk T and Seitsonen A P 2016 *Condens. Matter Phys.* **19** 23604
- [19] El Mendoub E B, Albaki R, Charpentier I, Bretonnet J-L, Wax J-F and Jakse N 2007 *J. Non-Cryst. Solids* **353** 3475
- [20] Kresse G and Hafner J 1993 *Phys. Rev. B* **48** 13115
- [21] Kresse G and Hafner J 1994 *Phys. Rev. B* **49** 14251
- [22] Kresse G and Furthmüller J 1996 *Comput. Math. Sci.* **6** 15
- [23] Kresse G and Joubert D 1999 *Phys. Rev. B* **59** 1758
- [24] Ceperley D M and Alder B J 1980 *Phys. Rev. Lett.* **45** 566
- [25] Perdew J P and Zunger A 1981 *Phys. Rev. B* **23** 5048
- [26] Bryk T and Wax J-F 2016 *J. Chem. Phys.* **144** 194501
- [27] Perdew J P, Burke K and Ernzerhof M 1996 *Phys. Rev. Lett.* **77** 3865
- [28] Allen M P and Tildesley D J 1989 *Computer Simulation of Liquids* (Oxford: Clarendon)
- [29] Smit B and Frenkel D 2002 *Understanding Molecular Simulations* 2nd edn (San Diego, CA: Academic)
- [30] Wax J-F, Bryk T and Jakse N 2020 to be published
- [31] Lin S-T, Blanco M and Goddard W A III 2003 *J. Chem. Phys.* **119** 11792